Supplemental Information for: Lightning Enhancement Over Major Oceanic Shipping Lanes

Joel A. Thornton[1], Katrina S. Virts[2], Robert H. Holzworth[3], and Todd P. Mitchell[4]

[1]Department of Atmospheric Sciences, University of Washington, Seattle, Washington

[2]NASA Marshall Space Flight Center, Huntsville, Alabama

[3]Department of Earth and Space Sciences, University of Washington, Seattle, Washington

[4]Joint Institute for the Study of the Atmosphere and Ocean, University of Washington, Seattle, Washington

Automatic Identification System (AIS) Ship Traffic and Emissions Inventory

Commercial marine vessels above a certain size use the Automatic Identification System (AIS) that repeatedly transmits via VHF information on a ship's heading, speed, size, type, country of origin, etc. This information can be received and recorded by ground-based networks or satellite sensors. An example of hourly global shipping activity from 2012 obtained by *exactEarth* using satellite AIS receivers can be found at www.shipmap.org. A snapshot is shown in Figure S1. Such data are not publicly available, and must be purchased. Some emissions inventory activities have purchased such data and these become the basis for aerosol particle emissions estimates shown in the manuscript (EDGAR database) [*Smith et al.*, 2014; *Crippa et al.*, 2016]. In situ observations of particle number size distributions, cloud condensation nuclei activitiy, composition, and optical properties from various ship types using a range of fuel compositions are expressed in terms of emission factors (*EF*): amount emitted per kg of fuel burned [*Hobbs et al.*, 2000; *Lack et al.*, 2009]. The emissions inventories are then a sum over such *EF* scaled by the fuel usage statistics derived from the shipping activity databases.

Estimate of CCN Enhancement in Indian Ocean Shipping Lane

To have an order-of-magnitude estimate of the impact of shipping on CCN in the region of enhanced lightning, we conduct the following simple calculation. The EDGAR emissions database predicts shipping leads to ~350 kg/km^2/yr of $PM_{2.5}$ emitted in the Indian Ocean shipping lane (see Figure 3c). *Lack et al*. [2009] find an *EF* ratio between CCN and PM_1 mass (sum of non-refractory sulfate, nitrate, ammonium, organic, and black carbon mass) of $EF_{CCN/PM}$ = 5x10^{14} g^{-1}. $EF_{CCN/PM}$ is the number of CCN (not CN) per gram of submicron particulate mass emitted. In a homogeneous volume, the time rate of change of CCN from shipping is therefore

$$\frac{d[CCN]}{dt} = \frac{E_{CCN}}{h} - \frac{1}{\tau}[CCN]$$

where E_{CCN} is the emission flux of CCN (km^{-2}/day), h is the mixed layer depth (km), and τ is the characteristic lifetime of CCN (day) in the region. Assuming a pseudo-steady state develops in the region due to the nearly constant shipping activity, then [CCN] from shipping can be calculated as

$$[CCN] = \frac{\tau E_{CCN}}{h}$$

Using an $E_{CCN} \sim 5\text{x}10^{17}$ km^{-2}/day, h of ~ 1 km, and τ ranging from 0.25 to 1-day due to transport and cloud scavenging, we find [CCN] from shipping alone would range from 100 to 500 cm^{-3} over the shipping lane. While very crude, these estimates are certainly large enough to conclude the shipping activity would be a significant perturbation to the background CCN typical of remote marine regions [*Ramanathan et al.*, 2001].

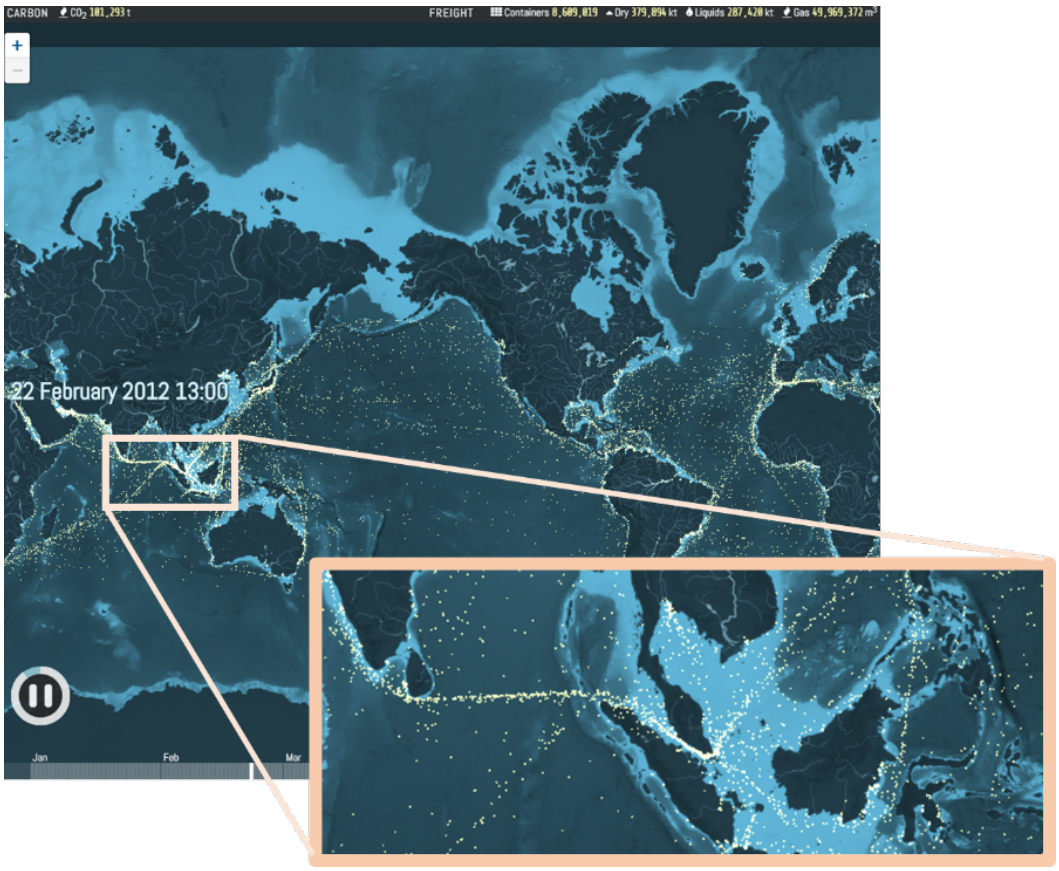

Figure S1. Example snapshot of global marine vessel traffic from February 22, 2012 obtained from www.shipmap.org. Data on ship position, heading and speed obtained from exactEarthTM satellite AIS data.

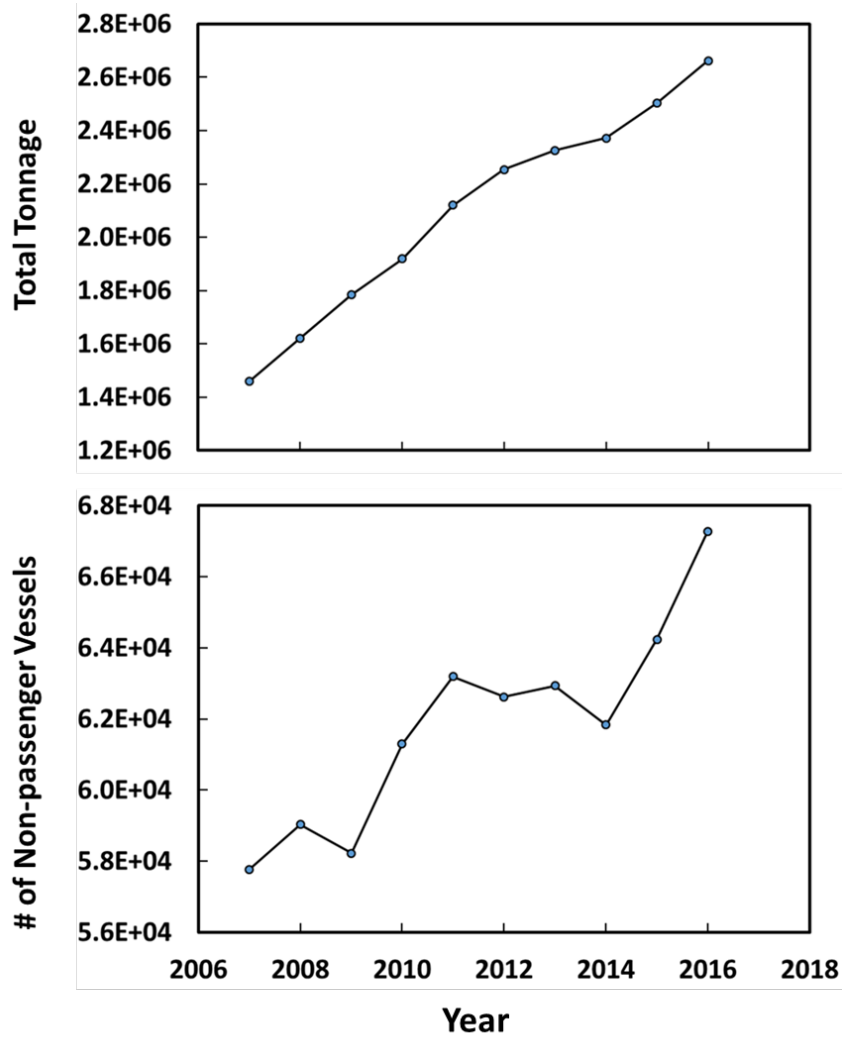

Figure S2. Maritime vessel arrivals into the port of Singapore in terms of total tonnage per year (top), and number of vessels excluding passenger and tugs (bottom), obtained from the Maritime Port Authority, Port of Singapore statistics (http://www.mpa.gov.sg/web/portal/home/port-of-singapore/port-statistics).

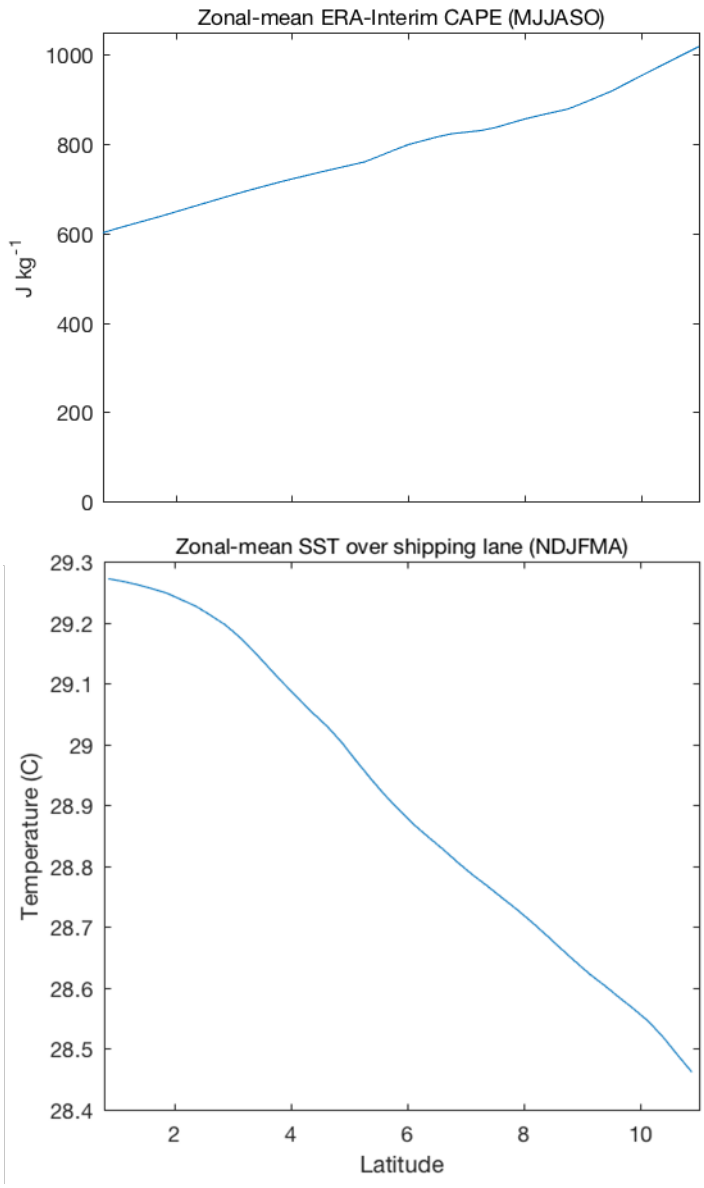

Figure S3. Top: seasonally averaged ERA-Interim Convective Available Potential Energy (CAPE) for northern hemisphere summer (MJJASO) for comparison with the northern winter mean shown in Figure 3d. Bottom: seasonally averaged sea surface temperature (SST) for northern hemisphere winter (NDJFMA) from the NOAA Optimal Interpolation (OI) SST daily, 0.25^{o} resolution dataset.

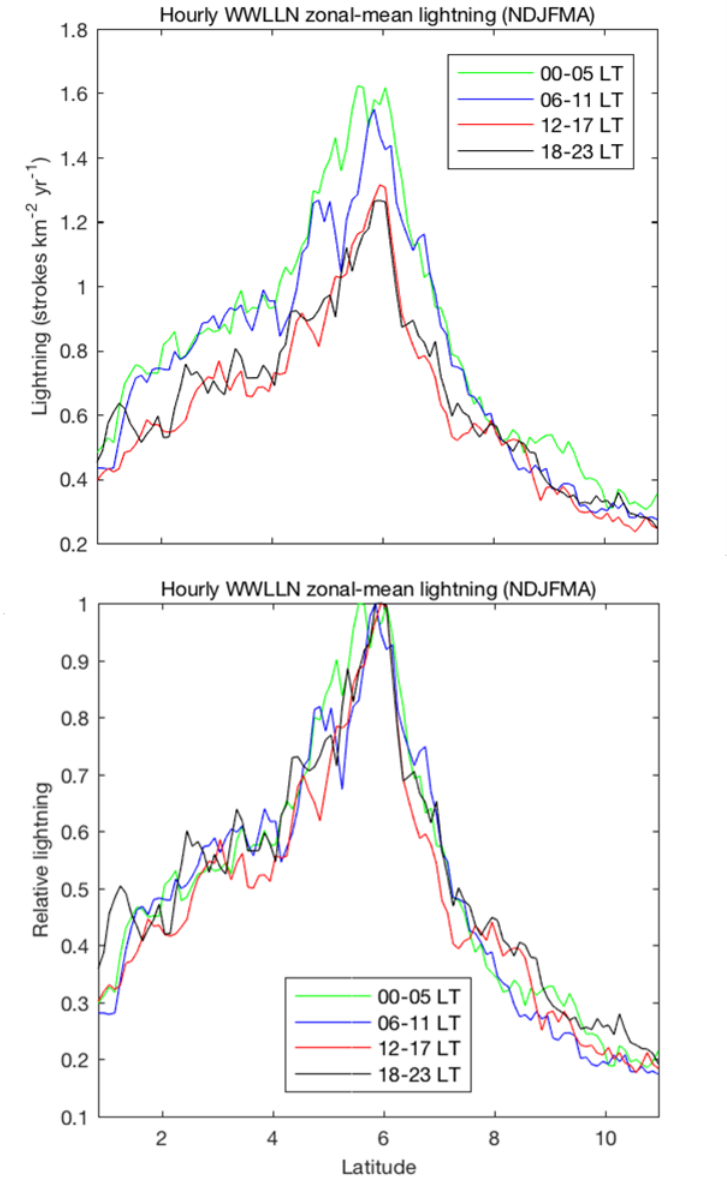

Figure S4. Absolute (top) and relative (bottom) hourly WWLLN lightning frequency during northern hemisphere winter (NDJFMA) is zonally averaged into four different local time of day bins for the same domain as in Figure 3. While there is a slight diurnal cycle in lightning frequency maximizing in the early morning, the enhancement over the shipping lane is persistent across all times of day and the relative magnitude of the enhancement has no apparent diurnal cycle.

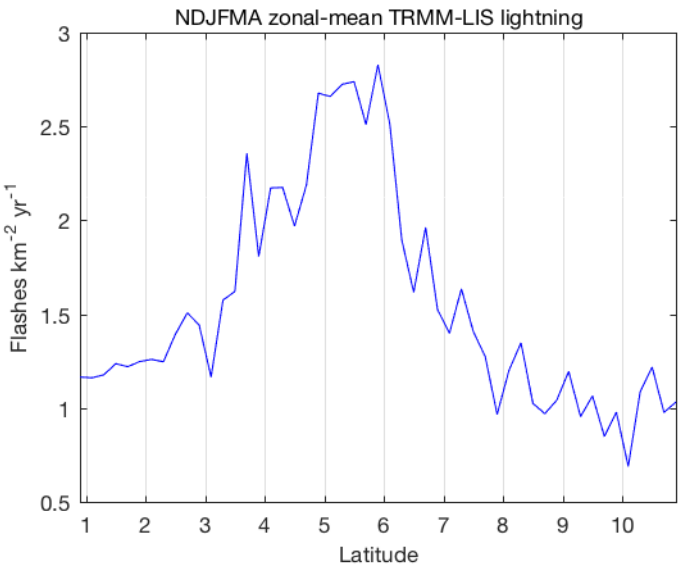

Figure S5. Zonal-mean lightning flash density from the TRMM-LIS satellite instrument (see text). All data collected during November - April from 1998 to 2015 over the same region in Figure 3 are used. The standard error of the mean (not shown) of the LIS flash density data shown in Figure S5 ranges between 0.25 and 0.35 flashes km^{-2} yr^{-1}. A somewhat broader enhancement is observed, possibly due to the much smaller sample size than the WWLLN data, which has an order of magnitude smaller standard error. The enhancement peaks between 5 to 6^{o}N and is nearly a factor of two over the surrounding region, similar to the enhancement detected with WWLLN.

We assume that meso and synoptic scale variations in the horizontal wind speed and direction together with more localized convective circulations disperse the ship plumes over hundreds of km in either direction. For example, a 3 m/s wind would advect the plume 260 km in 1 day. We are averaging lightning strokes over at least 2-year periods for this analysis, and thus we are making an average over the variations in wind direction and speed that occur on the daily and weekly timescales. The HYSPLIT gaussian dispersion model run for a few days in different months shows that indeed the plume from a single point source would advect 1^{o} or more, assuming a decay time for aerosol particles of several hours (see Figure S4). If we were to run such a calculation for a line source, more similar to the shipping lane, over several months, it is thus very likely the plume would be of order 1^{o} wide with a maximum at the source location.

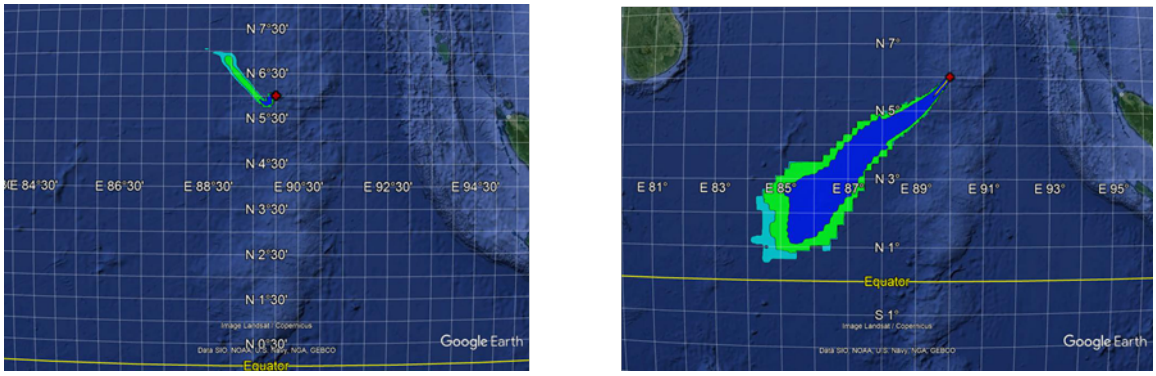

Figure S4. NOAA HYSPLIT Gaussian plume dispersion model results for a 350 kg/year source. Left Dec 18 - 19 2016 simulation. Right January 9 - 11 2016 simulation.

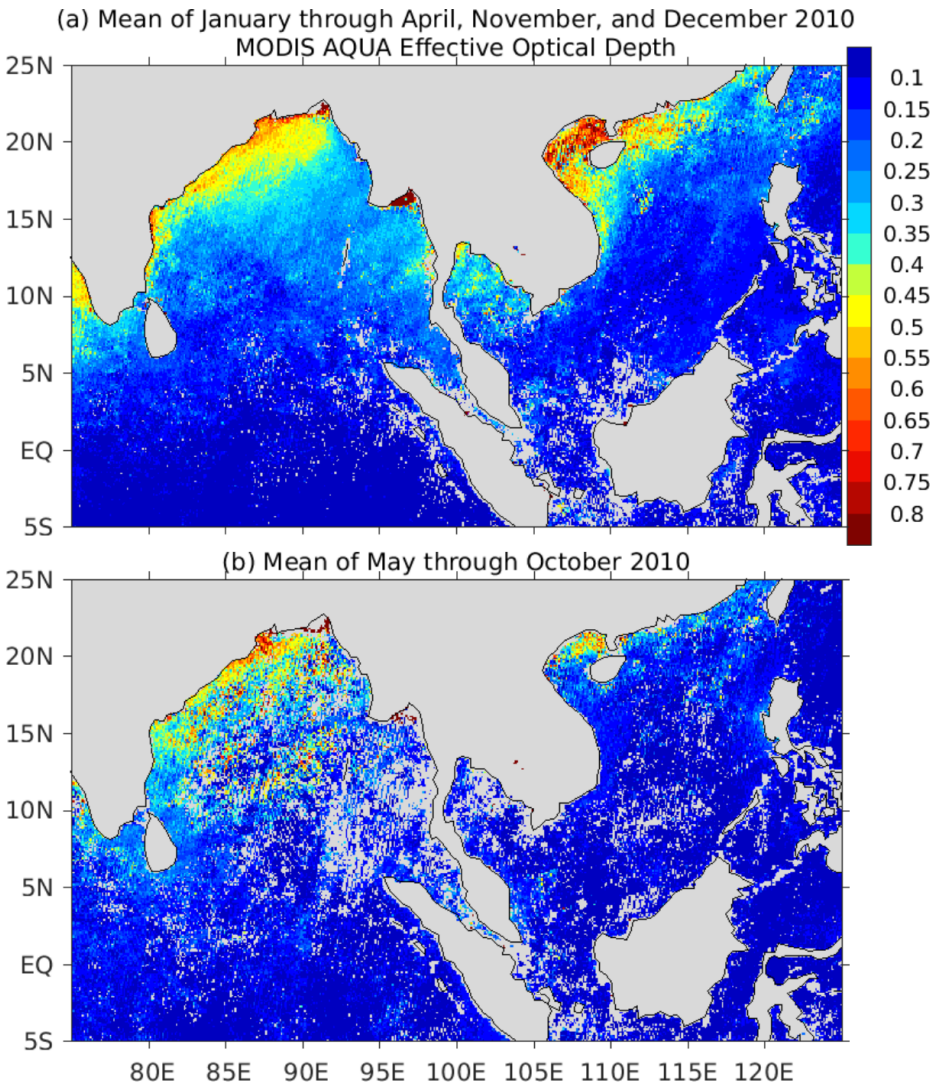

Figure S5. Aerosol optical depth (AOD) at 0.55 μm from the MODIS AQUA instrument over the same region as in Figure 1, averaged over January – April and November - December 2010 (a), and May – October, 2010 (b) . Only data where the cloud fraction (from the MODIS data set) was <10% are used in the averages.

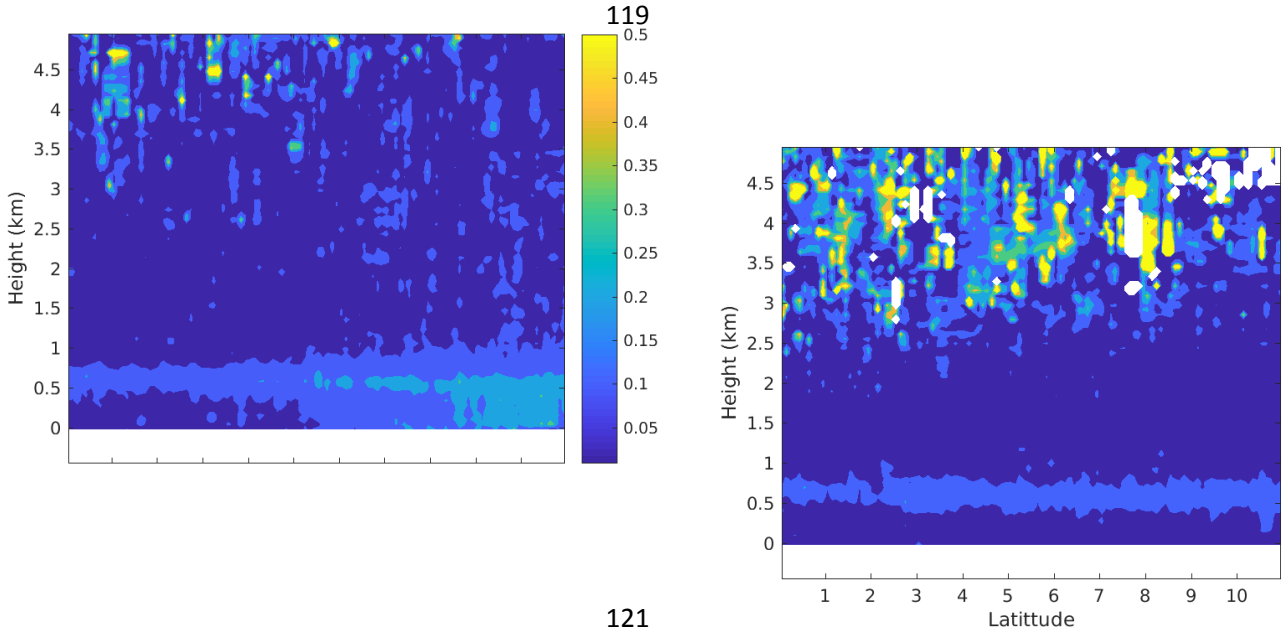

Figure S6. CALIOP aerosol extinction vertical profiles, averaged over the same region in Figure 3, for November through April (top) and May through October (bottom) 2006 – 2008. The layer of slightly enhanced aerosol extinction at 0.5 to 0.75 km throughout most the domain in both panels may be marine boundary layer cloud contamination of the aerosol signal. In the top panel, the elevated aerosol extinction north of 8^{o}N is likely pollution outflow from India into the Bay of Bengal and not associated with shipping.

References

Crippa, M., G. Janssens-Maenhout, F. Dentener, D. Guizzardi, K. Sindelarova, M. Muntean, R. Van Dingenen, and C. Granier (2016), Forty years of improvements in European air quality: Regional policy-industry interactions with global impacts, *Atmos. Chem. Phys.*, *16*(6),

3825–3841, doi:10.5194/acp-16-3825-2016.

Hobbs, P. V et al. (2000), Emissions from Ships with respect to Their Effects on Clouds, *J. Atmos. Sci.*, *57*(16), 2570–2590, doi:10.1175/1520-0469(2000)057<2570:EFSWRT>2.0.CO;2.

Lack, D. A. et al. (2009), Particulate emissions from commercial shipping: Chemical, physical, and optical properties, *J. Geophys. Res. Atmos.*, *114*(4), 1–16, doi:10.1029/2008JD011300.

Ramanathan, V., P. J. Crutzen, J. T. Kiehl, and D. Rosenfeld (2001), Aerosol, climate, and the hydrological cycle, *Science*, *294*(5549), 2119–2124, doi:10.1126/science.1064034.

Smith, T. W. P. et al. (2014), Third IMO Greenhouse Gas Study 2014, *Int. Marit. Organ.*, 327, doi:10.1007/s10584-013-0912-3, see also www.shipmap.org.